



ELSEVIER

Available online at [www.sciencedirect.com](http://www.sciencedirect.com)

SCIENCE @ DIRECT®

Surface and Coatings Technology 177–178 (2004) 447–452

**SURFACE  
& COATINGS  
TECHNOLOGY**

[www.elsevier.com/locate/surfcoat](http://www.elsevier.com/locate/surfcoat)

## Room temperature deposition of (Ti,Al)N and (Ti,Al)(C,N) coatings by pulsed laser deposition for tribological applications

J.M. Lackner<sup>a,b,c,\*</sup>, W. Waldhauser<sup>b</sup>, R. Ebner<sup>a,b</sup>, J. Keckés<sup>d</sup>, T. Schöberl<sup>d</sup>

<sup>a</sup>Materials Center Leoben, Franz-Josef-Strasse 13, A-8700 Leoben, Austria

<sup>b</sup>JOANNEUM RESEARCH, Laser Center Leoben, Leobner-Strasse 94, A-8712 Niklasdorf, Austria

<sup>c</sup>Institute of Physical Metallurgy and Materials Testing, University of Leoben, Franz-Josef-Strasse 18, A-8700 Leoben, Austria

<sup>d</sup>Erich Schmid Institute, Austrian Academy of Sciences, Jahnstrasse 12, A-8700 Leoben, Austria

### Abstract

Titanium–aluminium based nitride (Ti,Al)N and carbonitride (Ti,Al)(C,N) hard coating systems possess excellent tribological behaviour in metal cutting and polymer forming contacts. In the present work (Ti,Al)N and (Ti,Al)(C,N) coatings were deposited by employing the pulsed laser deposition (PLD) technique. A pulsed Nd:YAG laser with 1064 nm wavelength was used for the vaporization of TiAl targets in low-pressure N<sub>2</sub> or N<sub>2</sub>/C<sub>2</sub>H<sub>2</sub>, atmospheres at room temperature. The highly ionized metal vapour was deposited onto polished substrates (molybdenum, AISI D2). The coatings were characterized by light-microscopy, scanning electron microscopy, X-ray diffraction and hardness tests. The variation of the deposition parameters causes a change of the chemical composition, the texture and crystallinity of the coatings and, consequently, the mechanical properties and tribological behaviour. The latter was characterized in pin-on-disc tests at room temperature by using coated discs and uncoated AISI 52100 (DIN 100Cr6) steel and alumina pins as counterparts. The results demonstrate the excellent industrial applicability of these coatings for cold-forming operations: very low-wear rates were found for the (Ti,Al)N coatings. In contrast, the (Ti,Al)(C,N) coatings possess low-friction coefficients of approximately 0.2. As an outstanding advantage of these coatings, which were deposited at the room temperature by the PLD process, their excellent adhesion to the substrate can be pointed out, reaching the highest level (HF 1) in the Rockwell indentation test.

© 2003 Elsevier B.V. All rights reserved.

**Keywords:** Pulsed laser deposition; Laser ablation; Room temperature deposition; TiAlN; TiAlCN; Low wear; Low friction

### 1. Introduction

Hard material coatings are of continuously increasing interest for wear reduction of cold, hot and polymer forming tools as well as cutting tools. Titanium nitride (TiN), titanium carbide (TiC) and diamond-like carbon films are the most widely used coatings for these purposes [1], especially TiN is known because of its excellent tribological properties and the golden colour [1,2]. However, there are still several drawbacks such as hardness, adhesion, friction and oxidation resistance properties that limit the practical application of these coatings. In order to improve their properties, ternary coatings such as (Ti,Al)N and Ti(C,N) and quaternary coatings with additions of chromium, silicon, boron, etc. have been investigated in the last years. Among these,

the addition of aluminium to TiN in order to form a (Ti,Al)N ternary solid solution is attractive due to the significant enhancement of the oxidation resistance and the mechanical properties in comparison with TiN [2]. In addition, some authors [3–5] show an enhancement of the tribological properties by the addition of carbon to these ternary coatings.

The industrial manufacturing of hard coatings like (Ti,Al)N by physical vapour deposition (PVD), e.g. magnetron sputtering, ion plating and arc discharge deposition, or chemical vapour deposition (CVD) is well established nowadays [1]. But these techniques still have some disadvantages: (1) the limitation due to the thermal sensitivity of many substrates, e.g. TiN coatings are deposited by CVD at ~1000 °C and by PVD at >450 °C; and (2) space-charge problems for semiconductors and non-metallic substrates, e.g. polymers and other organic materials of high electrical resistance cannot be coated by most of the PVD/CVD methods.

\*Corresponding author. Tel.: +43-3842-402-730; fax: +43-3842-402-737.

E-mail address: [lacknerj@unileoben.ac.at](mailto:lacknerj@unileoben.ac.at) (J.M. Lackner).

Table 1  
Deposition parameters, film thicknesses, chemical compositions and hardnesses of the PLD (Ti,Al)(C,N) coatings T1–T5

Sample (coating)	Gas flow (deposition) (sccm)			Film thickness ( $\mu\text{m}$ )	Chemical composition			Hardness (GPa)
					Atomic ratio Ti/Al	N (at.%)	C (at.%)	
	N <sub>2</sub>	C <sub>2</sub> H <sub>2</sub>	Ar					
T1	15	–	15	1.5 $\pm$ 0.1	1.63 $\pm$ 0.05	31.1 $\pm$ 2.0	–	19.9 $\pm$ 0.4
T2	30	–	–	1.4 $\pm$ 0.1	1.38 $\pm$ 0.04	42.9 $\pm$ 1.9	–	32.2 $\pm$ 0.9
T3	45	–	–	1.5 $\pm$ 0.1	1.22 $\pm$ 0.06	47.5 $\pm$ 1.9	–	35.3 $\pm$ 1.3
T4	25	5	–	1.7 $\pm$ 0.1	1.05 $\pm$ 0.05	24.7 $\pm$ 1.4	24.7 $\pm$ 1.5	38.5 $\pm$ 1.5
T5	15	15	–	2.0 $\pm$ 0.1	1.06 $\pm$ 0.04	14.1 $\pm$ 2.2	36.5 $\pm$ 1.8	17.2 $\pm$ 0.4

Hence, there is a high demand for developing low-temperature deposition processes such as the pulsed laser deposition (PLD) for the growth of hard coatings on a broad variety of substrate materials [6–8].

In the PLD technique a pulsed laser beam is focussed onto a target in order to evaporate its surface layers under vacuum or low-pressure process gas atmospheres [9]. The vaporized material consisting of atoms, ions and atomic clusters is then deposited onto the substrate. The outstanding advantage of this technique is the possibility to deposit thin films of very high chemical purity and excellent adhesion on various substrate materials at room temperature. Furthermore, high rate film growth on surface areas placed perpendicular to the irradiated target surface is also possible by using a low-pressure gas. The application of reactive process gases gives the opportunity of varying the chemical composition of the films in a wide range.

The aim of the present paper was to study the applicability of the PLD process for the deposition of (Ti,Al)(C,N) films for tribological applications. Although some authors [10,11] have investigated the PLD of (Ti,Al)N coatings, no information is available about the tribological behaviour of such coatings as well as for (Ti,Al)(C,N) films.

## 2. Experimental

### 2.1. Film deposition

High purity Ti–Al targets (50 at.% Ti, 50 at.% Al) were taken for the ablation experiments using a pulsed Nd:YAG laser with 1064 nm wavelength, 0.8 J pulse energy and 10 ns pulse duration at a repetition rate of 10 Hz [12]. The targets were rotated during the laser irradiation in order to avoid the formation of deep craters. The emitted species were deposited at room temperature in argon and C<sub>2</sub>H<sub>2</sub> containing nitrogen atmospheres onto quenched and tempered cold working steel substrates (AISI D2) and molybdenum sheets with mirror-polished surfaces. The different atmospheres were chosen in order to produce (Ti,Al)N and (Ti,Al)(C,N) coatings with varying nitrogen and carbon contents (Table 1). Prior to the film deposition the substrates

were cleaned ultrasonically in pure acetone and subsequently in ethanol. To increase the adhesion to the substrate, TiAl adhesive interface layers have been deposited prior to the growth of the hard coating materials as recommended by Lii et al. [13].

### 2.2. Film characterization

The surface quality, the growth structures and the wear scars of the coatings were inspected with a light and a scanning electron microscope (Cambridge Instruments Stereoscan 360). The latter is equipped with an energy and a wavelength dispersive analyser (EDS and WDS) for chemical analysis. The phases of the (Ti,Al)(C,N) coatings were analyzed using an X-ray diffractometer (Siemens D500) and Cu K $\alpha$  radiation by  $\Theta/2\Theta$  scans in Bragg/Brentano arrangement (normal to the surface). Pole figure measurements were performed on a four cycle goniometer equipment (Seifert PTS 3000) with a step size of 2.5° for the polar and azimuthal angle.

The hardnesses and elastic moduli of the coatings were determined by nanoindentation with a Vickers indenter using a Fischerscope H100. The applied maximum load was approximately 10 mN, the loading rate was approximately 1 mN s<sup>-1</sup> for all measurements. The indentation depth ( $\sim$ 200 nm) was kept constant to prevent influences from the substrate and indentation size effects in testing the 1.4–2.0  $\mu\text{m}$  thick coatings.

The dry sliding friction behaviour of the coatings at room temperature (25 °C) and a relative humidity of 60% was evaluated using a CSEM Instruments high-temperature pin-on-disc tribometer with 6 mm AISI 52100 (DIN 100Cr6) bearing steel and Al<sub>2</sub>O<sub>3</sub> balls as counterparts. All experiments were carried out at a sliding speed of 0.1 m s<sup>-1</sup> on the as-deposited ultrasonically cleaned coating surfaces. The applied loads were 2 and 10 N for Al<sub>2</sub>O<sub>3</sub> and 100Cr6 counterparts, respectively. Optical profilometry (Veeco NT-1000) was used to inspect the wear tracks for analysing the wear mechanisms and the wear coefficients.

### 3. Results and discussion

#### 3.1. Film structure and chemical composition

Light and scanning electron microscopy (SEM) inspections of the as-deposited (Ti,Al)(C,N) coatings showed excellent film quality with only a small amount ( $\sim 15\,000\text{ mm}^{-2}$ ) of defects (droplets) of sub-micron size, originating from the ablation process of the target surface. SEM investigations on fracture sections were applied for determining the fracture morphology of the films and for measuring the film thicknesses after a deposition time of 60 min (Table 1). The deposition rates are similar to other PVD or CVD processes. The addition of  $\text{C}_2\text{H}_2$  to the process gas results in higher deposition rates (sample T4 and T5) due to more intensive scattering of the ablated species with  $\text{C}_2\text{H}_2$  molecules. The SEM investigations of the fracture sections revealed a micro-columnar film structure for the coatings T1–T4, which is comparable with Zone T structures of Thornton's structure zone model [14]. In contrast, a dense but amorphous-like structure was found for the coating T5. The possibility to get very dense microstructures of the hard coatings, even at low deposition temperatures, is one of the main advantages of the PLD process [6,8].

The chemical compositions of the coatings are shown in Table 1. The atomic Ti/Al ratio was found for all (Ti,Al)N coatings (T1–T3) much higher than that for the target (Ti/Al=1). This is likely due to differences in the re-sputtering rates of deposited Al and Ti atoms from the growing film surfaces. The nitrogen content increases with increasing  $\text{N}_2$  flow during deposition, but does not exceed 50 at.%, leading to excess (Ti,Al) contents. In contrast, the (Ti,Al)(C,N) coatings (T4, T5) have balanced, target-like Ti/Al atom ratios of approximately 1. The carbon content was found to be increased at the higher  $\text{C}_2\text{H}_2$  flow (coating T5) combined with a decrease of the (Ti,Al) content due to the easier ionization of the  $\text{C}_2\text{H}_2$  molecules and, thus, their higher reactivity during scattering with the evaporated species in the plasma.

The X-ray diffraction (XRD) investigations (Fig. 1) reveal for all samples with the exception of coating T5, a distinct crystallographic structure. Samples T1–T3 indicate the B1 NaCl structure of TiN, typical for the metastable  $(\text{Ti}_{1-x}\text{Al}_x)\text{N}$  phase [15,16]. Coating T1 shows in contrast to T2 and T3 a strongly preferred orientation with the (200) planes parallel to the film surface, which is confirmed by the texture analysis of this coating (Fig. 2a). In the case of coatings T2 and T3 the (220) planes are strongly preferred, leading to the (220) fiber texture (Fig. 2b). This difference can be attributed to the addition of argon to the process gas during deposition of coating T1. It is well known that an intensive bombardment of argon ions leads to the

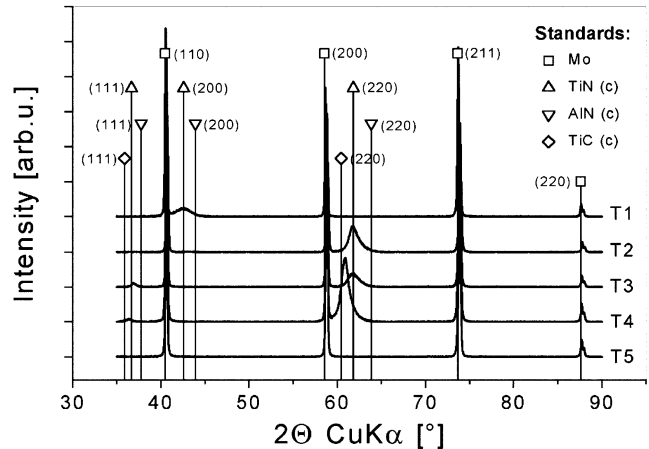


Fig. 1. XRD spectra of (Ti,Al)(C,N) coatings T1–T5 deposited onto Mo substrates. The standard positions of the main reflexions of molybdenum (Mo), titanium nitride (TiN), aluminium nitride (AlN) and titanium carbide (TiC) are indicated by different symbols.

'channeling' effect [17] of Ar ions in preferred crystallographic orientations of the growing film and, thus, to a minimization of the re-sputtering in distinct lattice planes. As a result, the film growth in this direction—for the fcc TiN structure it is the (200) direction—is preferred, leading to the (200) fiber texture. In contrast, the loss of the argon bombardment favours the growth of (111) and (220) planes because of the lower surface energies of these planes [18]. In addition, the lattice parameters of the (Ti,Al)N coatings T1–T3 are slightly smaller than that of the TiN standard. This phenomenon can be attributed to the replacement of titanium atoms by aluminium atoms in the fcc  $(\text{Ti}_{1-x}\text{Al}_x)\text{N}$  lattice [3]. Compared with the Al content of the films (Table 1), the observed shift is very small, which might be caused by the low nitrogen contents and residual compressive stresses, which affect the lattice spacings. These stresses are quite high for PLD hard coatings, which are grown at room temperature (e.g.  $\sim -8$  GPa for PLD TiN [6]), but have not been measured in the present work.

In contrast, a shift to lower diffraction angles and consequently larger lattice parameters can be observed for the (Ti,Al)(C,N) coating T4. The shift is large compared to the carbon content [19], which confirms again the presence of residual compressive stresses in this coating. The preferred orientation parallel to the surface of this coating is represented by the (220) planes, showing the nearly same fiber texture as coating T2.

The diffraction patterns of coating T5 reveal that no crystallographic phases are present except molybdenum of the substrate. These results are confirmed by the SEM analysis of the fracture sections. This behaviour is due to the very high carbon and hydrogen content,

incorporated in the coatings from the  $C_2H_2$  process gas during film growth.

### 3.2. Mechanical properties

Quantitative information about the adhesion of the coatings to the steel substrates was achieved by the Rockwell indentation method [20]. In all cases the highest adhesion class (HF 1) on a scale between HF 1 and HF 6 was determined, connected to very low cracking and no break-out areas around the indentation. The excellent adhesion of hard coatings is a further outstanding feature of the PLD process applied in this work caused by tough adhesive interfaces, e.g. shown in Refs. [6–8].

A tendency to higher hardness with increasing aluminium and nitrogen content (coating T1–T3) and low additions of carbon (T4) can be observed due to solid solution hardening [21,22] (Table 1). In contrast, a high carbon addition (coating T5) leads to a significant drop in hardness.

### 3.3. Tribological behaviour

Fig. 3 shows the coefficients of friction as a function of the sliding distance for the coatings T3 and T5 against a AISI 52100 (DIN 100Cr6) steel ball at room temperature and a humidity of approximately 60%. The shape of the curves was found typical for all sliding couples tested. During the run-in period (stage I) a significant increase from the initial friction coefficient at the first contact (0.2 and 0.4) to a maximum value

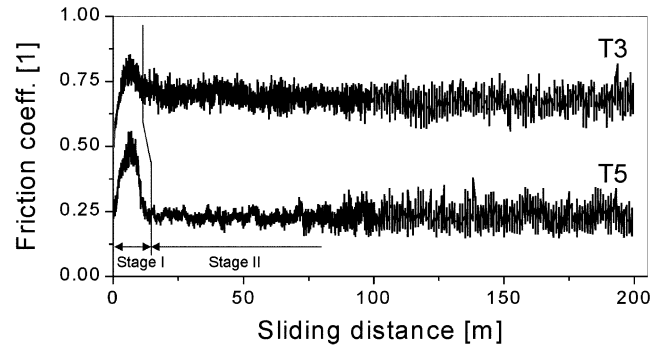


Fig. 3. Dependency of the friction coefficient on the sliding distance in the pin-on-disc test for the contact of AISI 52100 (DIN 100Cr6) steel pins and the coatings T3 and T5 (friction load: 10 N, sliding speed:  $0.1 \text{ m s}^{-1}$ , temperature:  $25 \text{ }^\circ\text{C}$ , relative humidity: 60%).

can be observed, which is followed by a drop to the steady-state friction coefficient in stage II. The first stage is characterized by the cracking of a few roughness tips of both counterfaces and, in the case of the 100Cr6 ball–(Ti,Al)N coating couple (T1–T3), the growth of a steel transfer layer on the coating's surface. This transfer layer is evident in stage II, too, and can be observed in optical profilometry imaging (Fig. 4a) as well as in EDS analysis performed in the wear tracks of the coatings. The EDS analysis reveals the presence of Ti, Fe, Cr, Al and O species. This confirms that apart from the material transfer an oxidation of the wear track during the sliding wear process occurs [23]. The growth of this transfer layer leads to mainly adhesive wear of the 100Cr6 counterpart ball and, thus, it is responsible

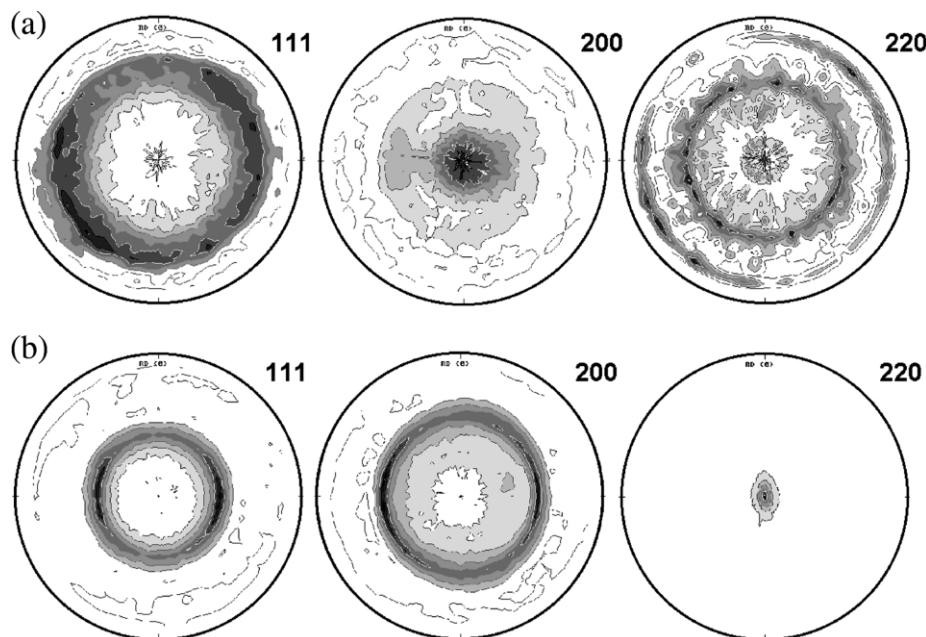


Fig. 2. Pole figures of the (1 1 1), (2 0 0) and (2 2 0) lattice planes of the (Ti,Al)N coatings (a) T1 and (b) T2 ( $\Psi=0\text{--}80^\circ$ ).

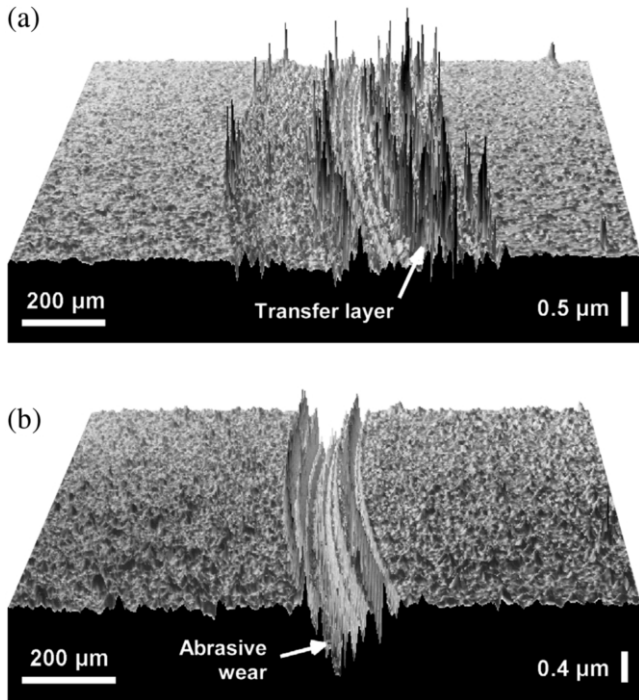


Fig. 4. Optical profilometry images of the wear tracks of coating (a) T3 and (b) T5 after sliding against AISI 52100 (DIN 100Cr6) steel counterparts (sliding distance: 200 m, friction load: 10 N, sliding speed:  $0.1 \text{ m s}^{-1}$ , temperature:  $25 \text{ }^\circ\text{C}$ , relative humidity: 60%).

for the high steady-state friction coefficients of approximately 0.7 (Fig. 5), which are in good accordance to Ref. [1]. The wear debris consists predominantly of work hardened and oxidised 100Cr6 material, which is ejected from the transfer layer during sliding. The disc wear rates of the (Ti,Al)N–100Cr6 couples are approximately one order of magnitude lower than the wear rates of PLD TiN–100Cr6 couples from a previous [6] as well as for sputtered (Ti,Al)N coatings [24], but in contrast the pin wear rates are very high. Furthermore, a significant dependency of the wear rates on the chemical composition and the hardness of the coatings can be observed. With increasing hardness of the coatings a lower coating wear rate and a higher counterpart wear rate were found.

In the case of the (Ti,Al)(C,N) coatings (T4, T5) sliding against 100Cr6 counterparts only abrasive wear of the coating was found (Fig. 4b). An EDS analysis of the counterpart revealed the existence of a transfer layer consisting of worn coating and ball material. The depths of the wear tracks on the coating surfaces and, thus, the wear volumes and wear rates, respectively, are approximately three times higher than that of the (Ti,Al)N films (Fig. 5) and are increasing with the carbon content. The wear rate of the sliding 100Cr6 pin is decreased for more than one order of magnitude due to the transfer layer formation on the pin. This transfer material is also

responsible for the low-friction coefficients of approximately 0.2–0.4 in the steady-state phase (stage II) (Fig. 5).

For the tribological contact of the (Ti,Al)N coatings (T1–T3) with alumina ( $\text{Al}_2\text{O}_3$ ) balls very high steady-state friction coefficients up to 1.0 were found. This high friction coefficient results from the lower applied friction loads (2 N) and the formation of highly abrasive wear debris leading to high friction forces because of the occurrence of ploughing wear in the wear track. Some ploughing wear scars were found in the optical profilometry investigations, but the general appearance of the wear tracks on the coating surfaces is very similar to Fig. 4b, showing only abrasive wear. The chemical analysis reveals the absence of a transfer layer due to the missing of titanium atoms on the wear scar of the alumina ball. The dependency of the wear rates on the coating hardness was found similar to the 100Cr6–(Ti,Al)N couple. A higher coating hardness leads to a

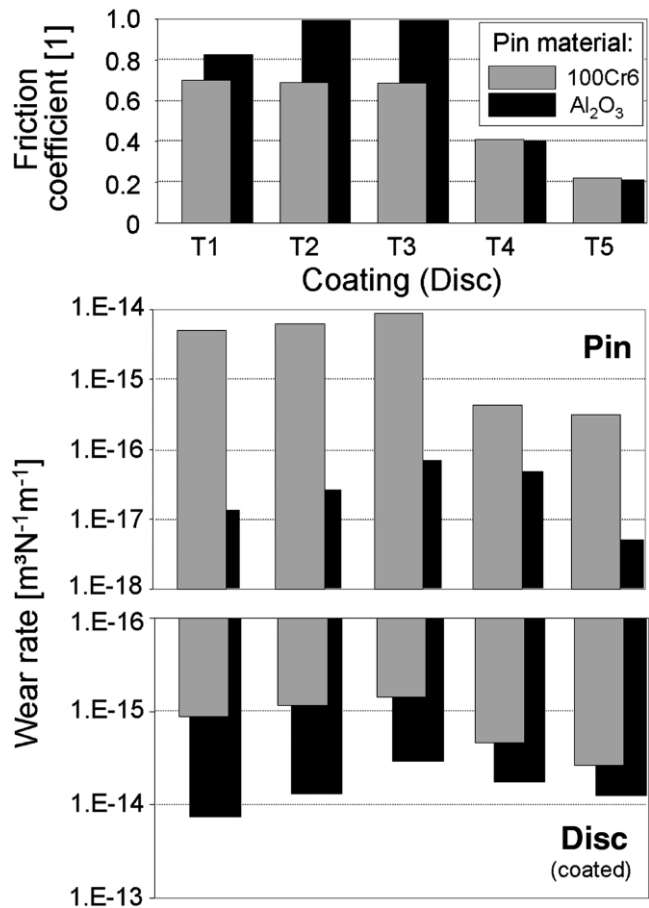


Fig. 5. Friction coefficients, pin and disc wear rates for the (Ti,Al)(C,N) coatings sliding against AISI 52100 (DIN 100Cr6) steel and  $\text{Al}_2\text{O}_3$  pins (sliding distance: 200 m, friction load: AISI 52100: 10 N,  $\text{Al}_2\text{O}_3$ : 2 N, sliding speed:  $0.1 \text{ m s}^{-1}$ , temperature:  $25 \text{ }^\circ\text{C}$ , relative humidity: 60%).

higher wear of the counterpart, but to a lower wear of the coating.

The influence of the carbon content of the coatings (coating T4, T5) on the tribological behaviour against  $\text{Al}_2\text{O}_3$  counterparts is also similar to the contact with 100Cr6 balls, described above. Only abrasive coating wear (mainly ploughing) has been found, the transfer layer formation is strongly reduced compared to the 100Cr6–(Ti,Al)(C,N) couples. As a result higher disc wear and lower pin wear in comparison to the  $\text{Al}_2\text{O}_3$ –(Ti,Al)N couples occur.

#### 4. Conclusions

Titanium–aluminum nitride (Ti,Al)N and carbonitride (Ti,Al)(C,N) coatings were deposited by the PLD technique at room temperature in  $\text{N}_2$  and  $\text{C}_2\text{H}_2$  containing atmospheres. Due to the outstanding features of the PLD technique high quality hard coatings with very smooth surfaces and excellent adhesion to the substrates (AISI D2 cold working steel) were fabricated. The chemical analyses revealed the possibility for the growth of coatings with varying Ti, Al, N and C contents. Except for the coatings with very high carbon contents all films were crystalline with a fiber textured microstructure, comparable to Thornton's dense and micro-columnar Zone T structure. The addition of Ar to the process gas causes a change from (2 2 0) to (2 0 0) textured coatings.

The tribological characterization, performed in unlubricated pin-on-disc tests at room temperature and a humidity of approximately 60%, revealed for both counterpart materials (100Cr6 ball bearing steel,  $\text{Al}_2\text{O}_3$ ) the same tendency: the higher the coating hardness the lower the coating wear rate and the higher is the counterpart wear rate. Generally, the wear rates of the (Ti,Al)N coatings are approximately one order of magnitude lower than that of PLD and PVD titanium nitride (TiN) coatings. Although the wear rates of the (Ti,Al)(C,N) are slightly higher, these coatings are of very high interest due to their low-friction coefficients ( $\sim 0.2$ ), which are up to five times lower than that of the (Ti,Al)N films sliding against 100Cr6 or  $\text{Al}_2\text{O}_3$  counterparts.

#### Acknowledgments

Financial support of this work by the Austrian Federal Ministry of Traffic, Innovation and Technology, the

Austrian Industrial Research Promotion Fund (FFF), the Government of Styria, the Technologie Impulse Gesellschaft mbH in the frame of the Kplus Programme and the European Union is highly acknowledged. The authors are grateful to Mrs R. Berghauser (Laser Center Leoben, JOANNEUM RESEARCH Forschungsgesellschaft mbH) and Mr M.H. Wong (The Hong Kong Polytechnic University, China) for preparing the coated samples at Laser Center Leoben.

#### References

- [1] K. Holmberg, A. Matthews, *Coatings Tribology*, Elsevier, Amsterdam, 1994.
- [2] C.-T. Huang, J.-G. Duh, *Surf. Coat. Technol.* 81 (1996) 164.
- [3] S. PalDey, S.C. Deevi, *Mater. Sci. Eng. A* 342 (2003) 58.
- [4] D. Heim, R. Hochreiter, *Surf. Coat. Technol.* 98 (1998) 1553.
- [5] K. Kawata, H. Sugimura, O. Takai, *Thin Solid Films* 390 (2001) 64.
- [6] J.M. Lackner, W. Waldhauser, R. Ebner, B. Major, T. Schöberl, Morphological, structural and tribological characterisation of pulsed laser deposited titanium nitride coatings, *Praktische Metallographie*, accepted.
- [7] J.M. Lackner, C. Stotter, W. Waldhauser, R. Ebner, W. Lenz, M. Beutl, *Surf. Coat. Technol.* 174–175 (2003) 402.
- [8] J.M. Lackner, W. Waldhauser, R. Ebner, W. Lenz, W. Mroz, *Galvanotechnik* 94 (2003) 1226.
- [9] D.B. Chrisey, G.K. Hubler, *Pulsed Laser Deposition of Thin Films*, Wiley, New York, 1994.
- [10] S. Acquaviva, E. D'Anna, L. Elia, *Thin Solid Films* 379 (2000) 45.
- [11] A. Morimoto, H. Shigeno, S. Morita, *Appl. Surf. Sci.* 127–129 (1998) 994.
- [12] R. Ebner, W. Waldhauser, W. Lenz, *Proceeding of Materials Week 2001*, Munich, 2001.
- [13] D.-F. Lii, J.-L. Huang, M.-H. Lin, *Surf. Coat. Technol.* 99 (1998) 197.
- [14] J.A. Thornton, *J. Vac. Sci. Technol.* 11 (1974) 666.
- [15] W.-D. Münz, *J. Vac. Sci. Technol. A* 4 (1986) 2717.
- [16] M. Pinkas, J. Pelleg, M.P. Dariel, *Thin Solid Films* 355–356 (1999) 380.
- [17] H. Lüth, *Surfaces and Interfaces of Solid Materials*, Springer, Berlin, 1995.
- [18] W. Ensinger, *Surf. Coat. Technol.* 65 (1994) 90.
- [19] L. Karlsson, L. Hultman, M.P. Johanson, *Surf. Coat. Technol.* 126 (2000) 1.
- [20] H. Jehn, G. Reiners, N. Siegel, *DIN-Fachbericht 39, Charakterisierung dünner Schichten*, Beuth-Verlag, Berlin, 1993.
- [21] C.-T. Huang, J.-G. Duh, *Surf. Coat. Technol.* 71 (1995) 259.
- [22] M. Zhou, Y. Makino, M. Nose, *Thin Solid Films* 339 (1999) 203.
- [23] S.-Y. Yoon, J.-K. Kim, K.H. Kim, *Surf. Coat. Technol.* 161 (2002) 237.
- [24] H. Ronkainen, K. Holmberg, K. Fancey, *Surf. Coat. Technol.* 43–44 (1990) 888.